

# Nano Science and Nano Technology

An Indian Journal

Full Paper

NSNTAJ, 9(3), 2015 [112-118]

## Photocatalytic activity of iron doped TiO<sub>2</sub> for indoor applications via Sol-Gel technique

Wesam A.A. Twej<sup>1\*</sup>, Ali H. Al-Hamdani<sup>2</sup>, AbdulKareem A. Al-Khafaji<sup>3</sup>, Falah H. Ali<sup>1</sup>

<sup>1</sup>Department of Physics, College of Science, University of Baghdad, Baghdad, (IRAQ)

<sup>2</sup>Department of Laser and Optoelectronic engineering, University of Technology, Baghdad, (IRAQ)

<sup>3</sup>Department of Physics, College of Education for pure Science/ Ibn Al-Haitham, University of Baghdad, Baghdad, (IRAQ)

E-mail: wesam961@yahoo.co.in

### ABSTRACT

Bare TiO<sub>2</sub> and Fe-doped TiO<sub>2</sub> films were prepared via Sol-Gel technique, and then deposited on glass substrates using dip-coating method. The characterizations for the prepared thin films were investigated by means of UV-VIS absorption, XRD, AFM and photo-degradation of Methylene Blue (MB) dye. The XRD measurement displays anatase phase in the prepared films. UV-VIS absorption spectra exhibited red shift in Fe-doped TiO<sub>2</sub> samples, whereas, AFM test demonstrates a decreasing in the root mean square roughness value in Fe-doped TiO<sub>2</sub> compared to that of bare sample. Finally, photocatalytic activity test shows that Fe-doped TiO<sub>2</sub> can be activated in the visible spectral region.

© 2015 Trade Science Inc. - INDIA

### KEYWORDS

Sol-gel;  
TiO<sub>2</sub> films;  
Photocatalytic activity;  
Thin films.

### INTRODUCTION

The field of heterogeneous photocatalysis has expanded rapidly within the last four decades, with various developments regarding energy and environment. Heterogeneous photocatalysis can be defined as the acceleration of photoreaction in the presence of a catalyst<sup>[1]</sup>. Most of the researches have been focused on TiO<sub>2</sub><sup>[2-4]</sup>, which shows relatively high reactivity and chemical stability under ultraviolet (UV) light, 387nm, whose energy exceeds the band gap of 3.2 eV in the anatase crystalline phase<sup>[1]</sup>. However, TiO<sub>2</sub> thin film exhibits superhydrophilicity under UV irradiation only.

Since UV irradiation participates only 5% of the

solar spectrum, it is preferable to extend the photocatalytic activity of TiO<sub>2</sub> to the visible spectral region which is the dominant spectral region of the solar spectrum in addition to the possibility of using it in indoor applications. This modification can be done by doping TiO<sub>2</sub> with metal ions<sup>[5-8]</sup>. Doping is the introduction of foreign elements into the parent photocatalyst without giving rise to a new crystallographic forms, phases or structures.

The band gaps (E<sub>g</sub>) as well as charge-carrier mobility are important in the photocatalytic activity of semiconductors<sup>[9-10]</sup>. It is well known that the CB and VB of TiO<sub>2</sub> are made up of Ti 3d and O 2p respectively<sup>[11]</sup>. The relationship between the electrode potential, (electrode potential conduction band

EPC and electrode potential valence band EPV), and ( $E_g$ ) for both conduction band minimum (CBM) and valence band maximum (VBM) can be approximately expressed by the following equations<sup>[11]</sup>

$$\text{EPC (vs. NHE)} = 1.23 - E_g \text{ (eV)}/2 \quad (1)$$

$$\text{EPV (vs. NHE)} = 1.23 + E_g \text{ (eV)}/2 \quad (2)$$

The ( $E_g$ ) for pure anatase  $\text{TiO}_2$  is 3.2eV, so the EPC and EPV are about  $-0.37 \text{ V}$  (vs. NHE) and  $+2.83 \text{ V}$  (vs. NHE) respectively. To achieve pollutants solar degradation, reduction ability of ( $e^-$ ) must be capable to produce super oxide acid ( $\text{HO}_2$ ) and super-oxide anion radicals ( $\text{O}_2^-$ ) as in equations (3 and 4). While oxidation of the photo generated holes ( $h^+$ ) must be able to oxidize  $\text{OH}^-$  to produce reactive hydroxyl radicals ( $\cdot\text{OH}$ ) according to equation (5)<sup>[12]</sup>.

The energy level at (CBM) is actually determines the reduction potential of photoelectrons. Whereas, the energy level at the (VBM) determines the oxidizing ability of photo-holes, each value reflecting the ability of the system to promote reductions and oxidations<sup>[13]</sup>.



Hui Yan *ital.* analyzed using the transition metals mono-doped in order to shift the  $\text{TiO}_2$  absorption into visible spectral range and improves its photocatalytic efficiency. He suggested that these cations as donors, which outer level (3d, 4d and 5d), should have higher atomic (d-orbital) energies than that of Ti to make sure that the CBM energy level is not lowered and high electron mobility is maintained<sup>[14]</sup>.

In this work, Fe doped  $\text{TiO}_2$  was studied under visible irradiation. The spectral modification of photocatalytic activity from UV to visible will extend the facility of application use to indoor as well as outdoor.

## EXPERIMENT

**Deionized water (18.2M $\Omega$ .cm), nitric acid ( $\text{HNO}_3$ ), purity 65%, from merck Co.**

Titaniumtetraisopropoxide (TTIP),  $\text{Ti} [\text{OCH}(\text{CH}_3)_2]_4$ , purity 97% and iron chloride ( $\text{FeCl}_3 \cdot 6\text{H}_2\text{O}$ ) from Sigma-Aldrich Co. were used as starting ma-

terials in sol-gel process. Several weights of iron chloride (0.0125, 0.0665, 0.1099 and 0.2205) gm were dissolved in water then mixed via the sol phase, yielding weight percentage mixing ratio of 2.21% (TF1), 6.40% (TF2), 10.16% (TF3) and 18.50% (TF4) respectively. One layer coating of bare  $\text{TiO}_2$  (T) and Fe-doped  $\text{TiO}_2$  (TF) was obtained by immersing the pre-cleaned substrates in the sol by dip-coating method using a dip-coater device, Dip coater unit Ho-TH-02, HDCM65, Korea. The substrate was kept in the sol for one minute to avoid the sol perturbations, and then it was withdrawn with a fixed speed of (3 mm/min). The substrate was dried in an oven for (10 minutes) at (80°C). Finally, the calcination was achieved in a furnace at (450°C) with a temperature rate of (20°C/min.) for three hours.

UV-Visible spectra were recorded using double beam (JASCO V-530) UV-Visible spectrophotometer in the absorption mode for the substrates. Atomic force microscope (AFM) was used to visualize the surface topography and surface roughness of the samples. The measurements utilized using (SPM) microscope in non-contact mode, made by (DME Co.), Dual scope model (DS95-200E). The crystalline phase was obtained by using diffractometer instrument from (STOE) Company/ Germany; model (STADI/MP).

Photocatalytic activity test was done by using (10ml) aqueous solution of methylene blue (MB) dye at concentration of ( $2 \times 10^{-5}$ ) [M] placed in a petri dish. Bare as well as Fe-doped  $\text{TiO}_2$  thin film samples were placed in this solution. Two types of exposure light were used; UV and visible light sources to degrade (MB) dye with bare and Fe-doped  $\text{TiO}_2$  thin film respectively. Both UV (200nm-400nm) and visible light (400nm-800nm) sources consist of three (6W) lamps were placed inside a suitable cabinet at a distance of (5cm) from the substrates. Representative samples of (MB) solution were taken at equal time intervals then measured their absorbance by spectrophotometer, fixed at wavelength of (564-574 nm), which represents the absorption peak value of the (MB) dye.

Hydrophilic behavior was evaluated by measuring the contact angle of a water droplet on the films using contact angle system from Dataphysics Com-

## Full Paper

pany/Germany) model (OCA/15 Plus).

### RESULTS AND DISCUSSION

The effect of Fe doping concentration on the structure of  $TiO_2$  films can be described by several tests.

#### XRD Test

The XRD patterns of Fe-doped  $TiO_2$  thin film, for two doping concentrations are shown in Figure (1). Five main distinguished peaks were mentioned in this Figure; (012, 101 004, 200 and 211), located in  $(2\theta)$  scale at (24, 26, 37, 47 and 56) respectively. The first one is related to  $(Fe_2O_3)^{[15]}$ , while the others are related to  $TiO_2$  anatase phase as denoted in

the scheme below the spectrum.

The XRD spectrum confirms that the anatase phase is dominated in the pattern, while the rutile phase was vanished. The excess of anatase phase in  $TiO_2$  film is favorable in photocatalytic applications<sup>[16-18]</sup>. Typically the XRD peak at low iron doping concentration, J.C. Yu et al<sup>[19,20]</sup>, is almost not distinguished. However, in this study, the peak fixed at  $(2\theta)$  equal to  $(24)$  which is related to (hkl) indices (012) was properly exist, this may be attributed to the, relatively, high doping Fe adopting concentration  $> 10\%$  weight percentage.

#### UV-visible absorption

Determination of the band gap gives an indication to the spectral response of bare  $TiO_2$  and  $TiO_2$

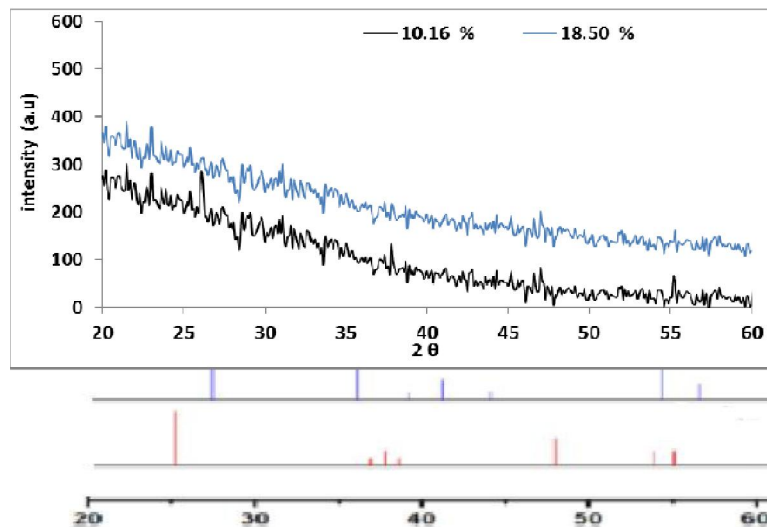


Figure 1 : X-ray diffraction pattern of Fe-doped  $TiO_2$  film at two different doping concentration

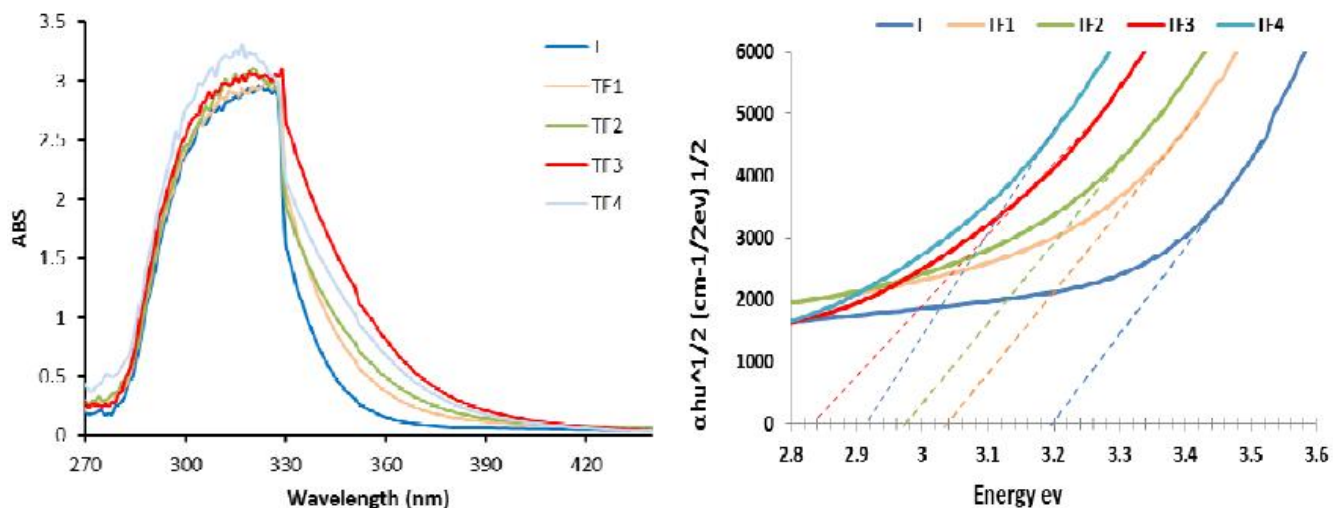


Figure 2 : (a) Absorption spectra, (b) band gap of bare  $TiO_2$  and Fe-doped  $TiO_2$  at several doping concentrations.

doped films. Figure (2) displays the UV-Visible absorption spectra for bare  $TiO_2$  and Fe-doped  $TiO_2$  samples. From this figure it is clear that the absorption edge was red shifted as the Fe additive concentration increases reaching maximum value at (10.16 %) then back to blue side. Tauc law gives the relation between the absorption coefficient ( $\alpha$ ) and photon energy ( $h\nu$ ) which can be written as  $[(\alpha h\nu) = (h\nu - E_b)^n]$  and can be used to obtain the energy gap, where (A) is absorption constant for indirect transitions<sup>[21]</sup>.

The iron is transition metal of (3d) outer level, the values of its CBM and VBM are (0.6 and 2.9) eV respectively, while for  $TiO_2$  the CBM and VBM are (-0.37 and 2.83) eV respectively<sup>[22]</sup>.

In fact, the CBM of  $Fe_2O_3$  is higher than that of  $TiO_2$ , this behavior will lead to increase the photocatalytic activity of the (Fe doped  $TiO_2$ ) samples in the visible region. The measured mobility for bare and Fe doped  $TiO_2$  samples were  $(0.67 \times 10^2$  and  $68.3 \times 10^2)$   $cm^2/(V.s)$  respectively. This significant increasing in the measured mobility may enhance the spectral shift to the red, i.e. visible spectral region, as suggested by Hui Yan *ital*.

The calculated band gap values of the prepared films were (3.2, 3.04, 2.97, 2.84 and 2.96 eV) for (T, TF1, TF2, TF3 and TF4) respectively. As a result the band gap energies of (Fe doped  $TiO_2$ )

samples were decreased as the (Fe) additive concentration increased, reaching minimum value at (10.16 %) then increased.

The difference in the band gap energies might be attributed to difference in the surface microstructure, composition and phase structure in  $TiO_2$  film after doping<sup>[23]</sup>.

This shift in the band gap can properly modify the photocatalytic response of the Fe-doped  $TiO_2$  films from its initial value 3.2 eV (387.5 nm) in the UV region to 2.84 eV (436 nm) in the visible region.

### AFM Test

The surface roughness of thin films was characterized by AFM. The surface texture can be tested by the height of their peaks, the depth of their valleys and the distance that separate peaks and valleys. The surface topography usually described in terms of surface roughness.

The AFM images of bare  $TiO_2$  (T) and Fe-doped  $TiO_2$  (TF) prepared samples are shown in Figure (3).

TABLE (1) illustrates three surface roughness parameters values; ratio of peak to valley ( $R_{p-v}$ ), the root mean square roughness ( $R_q$ ), and average roughness ( $R_{ave}$ )

The ( $R_{p-v}$ ) value decreases of about four times in (TF) samples compare to that of bare sample (T). While the ( $R_q$ ) and ( $R_{ave}$ ) values decreased five times.

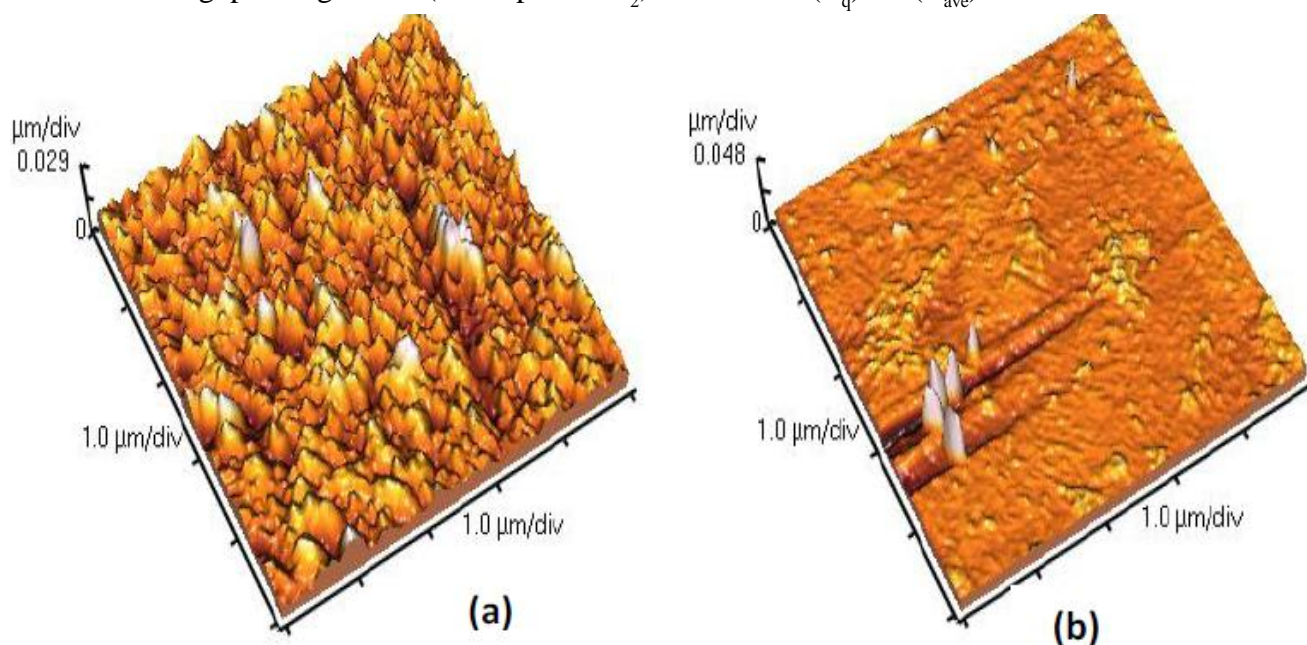


Figure 3 : AFM images of (a) bare  $TiO_2$  and (b) Fe-doped  $TiO_2$  thin film

## Full Paper

**TABLE 1 : Surface roughness parameters values from AFM measurement for bare and Fe doped  $\text{TiO}_2$  samples**

sample	$R_{p-v}$ (nm)	$R_q$ (nm)	$R_{ave}$ (nm)
T	122.6	10.37	6.44
TF	30.7	1.9	1.2

In this study, we adopted ( $R_{p-v}$ ) value since it is the nearest to the actual surface profile description. It is significant to notice that the average roughness can be the same for two surfaces, while their roughness profiles are totally different.

The reduction of ( $R_{p-v}$ ) after doping with iron chloride, i.e. the surface becomes smoother. This may give initial evidence that there is reduction in the surface to volume ratio after doping  $\text{TiO}_2$  film with  $\text{FeCl}_3$ . Obviously, large surface area and roughness offers greater number of activation centers which can fit on it, where the surface topography plays a crucial role in predicting catalytic properties<sup>[24]</sup>. However, this behavior will reduce the photocatalytic activity of the doped film but the goal of doping is to shift the spectral response from UV to visible light, which cannot be achieved by using bare film. This result will be confirmed by contact angle and photodegradation tests later.

### SEM observations

To investigate the influence of (Fe) doped  $\text{TiO}_2$ ;

the prepared samples images were analyzed. The outside image of bare sample, which is illustrated in Figure 4 (a), reveals that the film has regularly and well distributed surface structure even at magnified image Figure 4 (b). While in case of (Fe) doped  $\text{TiO}_2$  film image, the structure nature was somehow distinguished; clearly speaking we got granules located on different morphologies Figure 4 (c, d and e).

Meditate the SEM images, Figure (4d) shows that there are several scattered crystal shape, white color particles, that may be attributed to the presence of iron oxides ( $\text{Fe}_2\text{O}_3$  particles), which detected by XRD as well, within  $\text{TiO}_2$  structure. These ( $\text{Fe}_2\text{O}_3$ ) particles seemed to be distributing mostly over the surface of the host and lay closely together with  $\text{TiO}_2$  matrices. The (Fe) ions may play significant roles in modification the surface morphology, then the surface area topography.

We believe that this modification in surface area will create different intramolecular fields which may agitate the conductive band of  $\text{TiO}_2$  matrices, i.e. broadening it, and then decreasing its minimum conductive band (MCB) value. Furthermore the (Fe) dopant will enhance the indirect transitions yielding new composite especially at higher doping concentration  $\approx 10$  weight %.

### Photocatalytic activity test

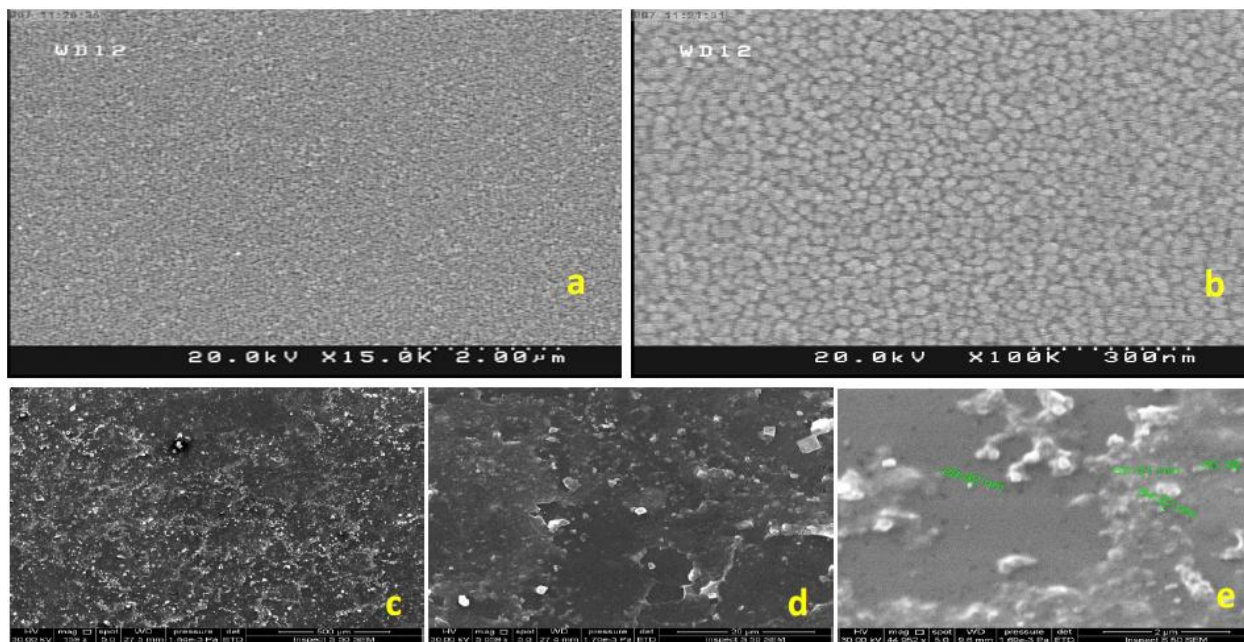


**Figure 4 : SEM micrographs of (a) bare  $\text{TiO}_2$  and (b) Fe-doped  $\text{TiO}_2$  thin film**

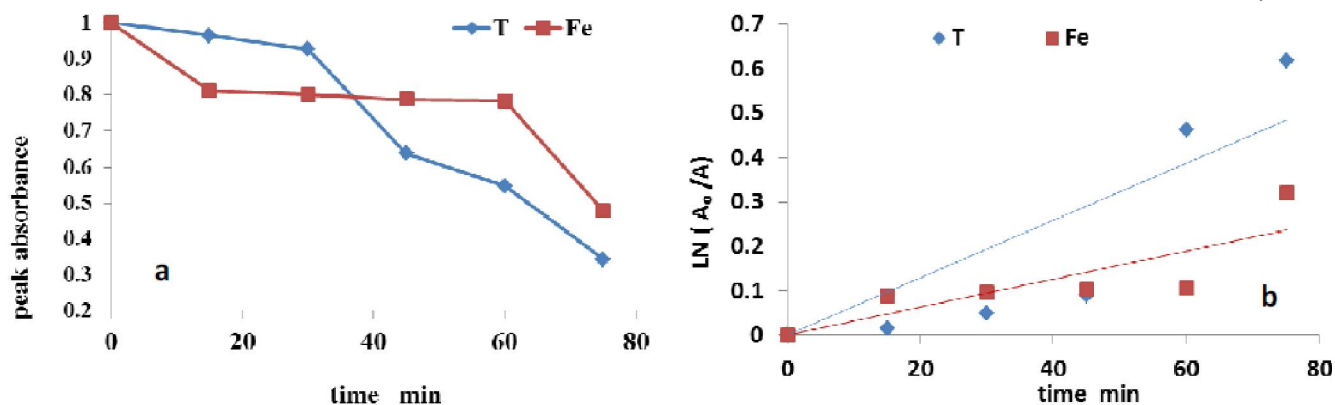


**Figure 5 :** Photocatalytic activity for bare TiO<sub>2</sub> under UV exposure and Fe-doped TiO<sub>2</sub> under visible light (a) MB absorbance fixed at the wavelength of (564-574) nm vs. exposure time (b) Ln initial absorbance over test absorbance ( $A_0/A$ ) vs. exposure time

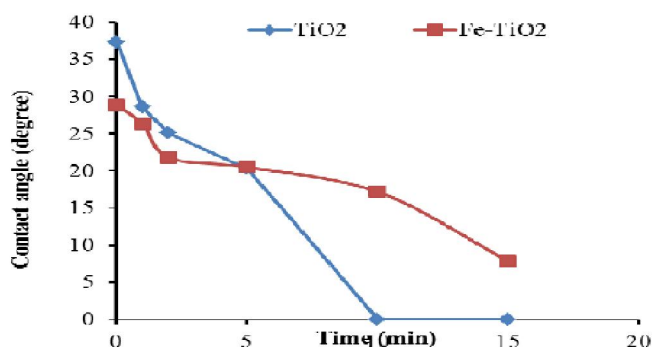


**Figure 6 :** Contact angle versus exposure time for bare TiO<sub>2</sub> under UV exposure and Fe-doped TiO<sub>2</sub> under visible light

The photocatalytic activity test reveals that (Fe) doped TiO<sub>2</sub> act as photocatalyst even when it is illuminated by visible light. In spite of the degradation of visible light in this case is lower than in the case of UV light exposure, but it is still effective. However, after one hour the (MB) absorbance was reduced to its half initial value. A graph between the absorbance versus UV and visible irradiation time intervals in minutes was plotted as shown in Figure (5).

Figure (6) shows the difference in hydrophilicity between bare films, under UV exposure, and (Fe) doped TiO<sub>2</sub> film under visible light.

Both films exhibit hydrophilic property, where after (10 min.) of UV exposure time the bare film exhibits totally hydrophilic (superhydrophilicity), while the contact angle of (Fe) doped TiO<sub>2</sub> film was reduced to its quarter initial value after (15 min.) of visible exposure time. This response of the modified film to the visible light may extend its facility to

the indoor applications.

## CONCLUSION

TiO<sub>2</sub> and (Fe) doped TiO<sub>2</sub> nanoparticles were successfully synthesized via Sol-gel technique using Titanium tetraisopropoxide (TTIP) as a precursor. By using this technique totally anatase phase can be exhibited in the thin film which confirmed by XRD measurements. Doping iron chloride in titanium oxide matrices initiate red shifting in the absorption edge. Thus, subsequently; decreases the band gap energies of the TiO<sub>2</sub> samples. The doping concentration play significant roles in determination the final band gap achieve value. The results presented by AFM illustrate that the TiO<sub>2</sub> thin film surface roughness was decreased after Fe doping. Photodegradation activities as well as hydrophilicity in the visible region were accomplished merely by suitable doping concentration of iron.

## REFERENCES

- [1] A. Fujishima, K. Honda; Electrochemical photolysis of water at a semiconductor electrode, *Nature*, **238**, 37, 37-38 (1972).
- [2] K.I. Hadjiivanov, D.K. Klissurski; Surface chemistry of titania (anatase) and titania-supported catalysts", *Chem. Soc. Rev.*, **25**, 1, 61-69 (1996).
- [3] J. Schneider, M. Matsuoka, M. Takeuchi, J. Zhang, Y. Horiuchi, M. Anpo, D.W. Bahnemann; Understanding TiO<sub>2</sub> Photocatalysis: Mechanisms and Materials, *Chem. Rev.*, **114**, 19, 9919-9986 (2014).

## Full Paper

- [4] J.Cai, Y.Zhu, D.Liu, M.Meng, Z.Hu, Z.Jiang; Synergistic effect of titanate-anatase heterostructure and hydrogenation-induced surface disorder on photocatalytic water splitting, *ACS Catal.*, **5**, 3, 1708–1716 (2015).
- [5] A.K.Eshaghi; Am.Eshaghi, Optical and hydrophilic properties of Cr doped TiO<sub>2</sub>-SiO<sub>2</sub> nanostructure thin film, *Appl.Surf.Sci.*, **258**, 7, 2464-2467 (2012).
- [6] K.Hashimoto, H.Irie, A.Fujishima; TiO<sub>2</sub> photocatalysis: A historical overview and future prospects, *JJAP*, **44**, 12, 8269–8285 (2005).
- [7] J.C.Yu, Jiaguo, Wingkei, Zitao, Lizhi; Effects of F-doping on the photocatalytic activity and microstructures of nanocrystalline TiO<sub>2</sub> powders, *Chem.Mater.*, **14**, 9, 3808–3816 (2002).
- [8] S.Banerjee, S.C.Pillai, P.Falaras, K.E.O'Shea, J.A.Byrne, D.D.Dionysiou; New insights into the mechanism of visible light photocatalysis, *J.Phys.Chem.Lett.*, **5**, 15, 2543–2554 (2014).
- [9] P.R.Mishra, P.K.Shuklab, O.N.Srivastava; Study of modular PEC solar cells for photoelectrochemical splitting of water employing nanostructured image photoelectrodes, *Int.J.of Hydrogen Energy*, **32**, 1680–1685 (2007).
- [10] S.U.M.Khan, M.Al-Shahry, S.Zhou; Efficient photochemical water splitting by a chemically modified n-TiO<sub>2</sub>, *Science*, **297**, 5590, 2243–2245 (2002).
- [11] R.Abe, K.Sayama, H.Arakawa; Significant effect of iodide addition on water splitting into H<sub>2</sub> and O<sub>2</sub> over Pt-loaded TiO<sub>2</sub> photocatalyst: Suppression of backward reaction, *Chem.Phys.Lett.*, **371**, 360–364 (2003).
- [12] D.Dvoranová, V.Brezová, M.Mazúra, M.A.Malati; Investigations of metal-doped titanium dioxide photocatalysts, *Appl.Catal.B Environmental*, **37**, 91–105 (2002).
- [13] O.Carp, C.L.Huisman, A.Reller; Photo induced reactivity of titanium dioxide, *Progress in Solid State Chemistry*, **32**, 33-177 (2004).
- [14] H.Yan, X.Wang, M.Yaon, X.Yao; Band structure design of semiconductors for enhanced photocatalytic activity: The case of TiO<sub>2</sub>, *Progress in Natural Science: Materials International*, **23**, 4, 402–407 (2013).
- [15] M.C.Morris, H.F.McMurdie, E.H.Evans, B.Paretzkin, H.S.Parker, N.C.Panagiotopoulos; Standard X-ray diffraction powder patterns section 18 data for 58 substances, **37**, (1981).
- [16] T.Luttrell, S.Halpegamage, J.Tao, A.Kramer, E.Sutter, M.Batzill; Why is anatase a better photocatalyst than rutile? - Model studies on epitaxial TiO<sub>2</sub> films, *Nature.com Scientific Reports*, **4**, 4043, 1-7 (2014).
- [17] D.Vernardou, G.Kalogerakis, E.Stratakis, G.Kenanakis, E.Koudoumas, N.Katsarakis; Photo-induced hydrophilic and photocatalytic response of hydrothermally grown TiO<sub>2</sub> nanostructured thin films, *Solid State Sciences*, **11**, 1499–1502 (2009).
- [18] A.Molea, V.Popescu; The obtaining of titanium dioxide nanocrystalline powders, *Opto.and adv.materials-Rapid Commu.*, **5**, 3, 242-246 (2011).
- [19] J.Yu, J.Xiong, B.Cheng, S.Liu; Fabrication and characterization of Ag-TiO<sub>2</sub> multiphase nanocomposite thin films with enhanced photocatalytic activity, *Appl.Catal.B* **60**, 3-4, 211-221 (2005).
- [20] J.C.Yu, J.Yu, W.Ho, J.Zhao; Light-induced superhydrophilicity and photocatalytic activity of mesoporous TiO<sub>2</sub> thin films, *Journal of Photochemistry and Photobiology A: Chemistry*, **148**, 331-339 (2002).
- [21] W.Y.Teoh, R.Amal, L.Mädler, S.E.Pratsinis; Flame sprayed visible light-active Fe-TiO<sub>2</sub> for photomineralisation of oxalic acid, *Catal.Today*, **120**, 2, 203 213 (2007).
- [22] M.Toroker, D.K.Kanan, N.Alidoust, L.Y.Isseroff, P.Liaob, E.A.Carter; First principles scheme to evaluate band edge positions in potential transition metal oxide photocatalysts and photoelectrodes, *Phys.Chem.Chem.Phys.*, **13**, 16644–16654 (2011).
- [23] K.Naeem, F.Ouyang; Preparation of Fe<sup>3+</sup>-doped TiO<sub>2</sub> nanoparticles and its photocatalytic activity under UV light, *Physica B.*, **405**, 1, 221 226 (2010).
- [24] M.Aronniemi, J.Lahtinen, P.Hautojarvi; Characterization of iron oxide thin films, *Surf.Interface Anal.*, **36**, 1004–1006 (2004).